NATIONAL ADVISORY COMMITTEE FOR AERONAUTICS

TECHNICAL NOTE

No. 1689

LOAD DISTRIBUTIONS DUE TO STEADY ROLL AND PITCH FOR THIN WINGS AT SUPERSONIC SPEEDS

By W. E. Moeckel and J. C. Evvard

Flight Propulsion Research Laboratory
Cleveland, Ohio

Washington
August 1948

NATIONAL ADVISORY COMMITTEE FOR AERONAUTICS

TECHNICAL NOTE No. 1689

LOAD DISTRIBUTIONS DUE TO STEADY ROLL AND PITCH FOR THIN WINGS AT SUPERSONIC SPEEDS

By W. E. Moeckel and J. C. Evvard

SUMMARY

A method is presented for determining the load distribution due to steady roll and pitch for thin flat-plate wings whose plan form is arbitrary except that a part of the leading edge must be supersonic.

For wings with straight supersonic leading edges, the load distributions due to angle of attack, steady roll, and steady pitch are explicitly evaluated and are computed for a family of wings whose plan form includes most types of flow region commonly encountered. These computations showed that negative lift existed toward the rear of pointed wings whose aspect ratio was small. In steady roll, negative loading occurred in regions influenced by the edge of the plan form at the opposite side of the roll axis. When the pitch axis was located near the semichord position, the load gradient for steady pitch was approximately in the chordwise direction, except in regions influenced by subsonic trailing edges. High positive loading occurred toward the front of the wing and high negative loading toward the rear.

INTRODUCTION

A method is presented in reference 1 for determining the pressure distribution over thin wings at supersonic speeds. The method is based on an integration of the local source strength (which is proportional to the local slope of the wing surface) over the regions of the disturbed flow field that lie within the forward Mach cone from a point on the wing surface. Reference 1 shows that the contributions to the pressure coefficient of the disturbed fields off the surface of the wing may be replaced by equivalent contributions of parts of the wing surface, and that some of the surface integrals that are involved in the determination of pressure coefficient may be reduced to line integrals.

The reduction of surface integrals to line integrals is feasible for all regions of a flat-plate wing except those influenced by

interacting disturbed flow fields off the wing plan boundary. For the wing shown in figure 1, for example, all regions may be treated by the methods of reference 1 except the small shaded regions at the rear. The restriction that a portion of the leading edge must be swept ahead of the Mach lines from the foremost point of the wing thus guarantees that some portions of the wing will be subject to the methods of reference 1. For regions influenced by interacting disturbed flow fields, more elaborate methods are required, such as those used for delta wings in reference 2.

The load distributions due to roll and pitch have been determined for some plan forms with straight edges in references 3 and 4. The methods of reference 1 are applied herein to the determination of these load distributions for more general classes of plan form, whose edges may be curved. For a family of wings of the type shown in figure 1, but having, for convenience, straight supersonic leading edges, the load distributions due to angle of attack, steady roll, and steady pitch were computed. This type of wing was chosen because it contains most types of flow field commonly encountered.

This analysis was completed at the NACA Cleveland laboratory during January 1948.

SYMBOLS

The following symbols, some of which are illustrated in figure 2 to 6, are used throughout this report:

A, B, C_1, C_2, . . ., C_{10}	substitution terms
a, a', b, b', c, c'	integration limits
C_p	pressure coefficient
k	slope of straight leading edge in (u,v) coordinate system
M	Mach number
p	steady rate of roll, radians per second
q	steady rate of pitch, radians per second

S	area or area integration
S_w	area on wing surface
U	free-stream velocity (in x-direction)
u, v	variables of integration in oblique coordinates
u_w, v_w	oblique coordinates of point on wing surface
u_d, v_d	oblique coordinates of wing vertex
$u_1(v)$, $v_1(u)$, $y_1(x)$	functions defining form of right supersonic leading edge
$u_2(v)$, $v_2(u)$, $y_2(x)$	functions defining form of left supersonic leading edge
$u_3(v)$, $v_3(u)$, $y_3(x)$	functions defining form of right subsonic leading and trailing edges
$u_4(v)$, $v_4(u)$, $y_4(x)$	functions defining form of left subsonic leading and trailing edges
w	component of perturbation velocity in z-direction (positive outward from $z = 0$ plane)
x, y	Cartesian coordinates of point on wing surface
ξ, η	variables of integration in Cartesian coordinates
η_0	coordinate of roll axis
ξ_0	coordinate of pitch axis
α	angle of attack
$\beta = \sqrt{M^2 - 1}$	
σ_T, σ_B	w/U for top and bottom wing surface, respectively, in y = constant plane

ANALYSIS

A plan form that contains most types of wing region commonly encountered is shown in figure 1. The downstream Mach lines from the vertex and from the junctures of the subsonic and supersonic sections of the leading edges divide the plan form into nine types of region that differ in the type and number of wing edges that affect the pressure distribution. Regions I and II are influenced only by supersonic leading edges, whereas regions III, IV, and V are affected also by one subsonic leading or trailing edge. In regions VI, VII, and VIII, the subsonic edges of both sides of the wing affect the flow. The shaded areas represent regions that are affected by interacting perturbed fields off the wing plan form and are not easily treated by the methods of reference 1.

The essential equations required to determine the load distribution for the type of wing shown in figure 1 (without the shaded regions) may be obtained from a consideration of regions of types III, IV, and V. For these types of region (influenced by supersonic leading edges and only one subsonic leading or trailing edge), an expression was derived in reference 1 for the pressure coefficient at a point (x,y) when that point is not influenced by vorticity off the wing plan-form boundary. This expression is (see fig. 2):

$$C_p = \frac{2}{\pi}\iint_{S_{w,1}} \frac{\frac{\partial \sigma_T}{\partial \xi}\, d\xi d\eta}{\sqrt{(x-\xi)^2 - \beta^2(y-\eta)^2}} + \frac{2}{\pi}\iint_{S_{w,2}} \frac{\frac{\partial(\sigma_B + \sigma_T)}{\partial \xi}\, d\xi d\eta}{2\sqrt{(x-\xi)^2 - \beta^2(y-\eta)^2}}$$

$$+ \frac{2}{\pi}\int_{\overline{ab}} \frac{\sigma_T d\eta}{\sqrt{(x-\xi)^2 - \beta^2(y-\eta)^2}} + \frac{2}{\pi}\int_{\overline{bOd}} \frac{(\sigma_B + \sigma_T)\, d\eta}{2\sqrt{(x-\xi)^2 - \beta^2(y-\eta)^2}}$$

$$+ \frac{2}{\pi}\int_{\overline{bd}} \frac{\beta\left(\frac{dy}{dx}\right)_3 (\sigma_T - \sigma_B)\, d\eta}{\left[1 + \beta\left(\frac{dy}{dx}\right)_3\right]\sqrt{(x-\xi)^2 - \beta^2(y-\eta)^2}} \qquad (1)$$

where $\left(\frac{dy}{dx}\right)_3$ is the derivative of the equation defining the plan form of the subsonic leading and trailing edges evaluated at the intersection of the right forward Mach line from (x,y) and the wing boundary (point d). Equation (1) was shown in reference 1 to contain an additional term of a form similar to the line integral along the Mach line $\overline{bd}$. This additional line integral is related to the vorticity behind the trailing edge and is therefore zero for leading edges. For trailing edges, the nature of the line integral depends on the conditions imposed. In particular, if the Kutta-Joukowski condition is imposed, the additional line integral must be such that it exactly cancels the integral along the Mach line $\overline{bd}$. Hence, equation (1), without the last integral, can be used to determine the pressure coefficient in regions influenced by vorticity off the plan form provided that the Kutta-Joukowski condition is imposed at subsonic trailing edges. The imposition of this condition, although arbitrary, is conventional and will be assumed in the rest of the analysis.

For a flat-plate wing, the effective local slopes σ_B and σ_T for determining the loading due to angle of attack, steady roll, and steady pitch, are

$$\left.\begin{aligned} \sigma_T &= -\alpha \\ \sigma_B &= \alpha \end{aligned}\right\} \tag{2}$$

$$\left.\begin{aligned} \sigma_T &= -\frac{w}{U} = -\frac{p}{U}(\eta - \eta_0) \\ \sigma_B &= \frac{p}{U}(\eta - \eta_0) \end{aligned}\right\} \tag{2a}$$

$$\left.\begin{aligned} \sigma_T &= -\frac{w}{U} = -\frac{q}{U}(\xi - \xi_0) \\ \sigma_B &= \frac{q}{U}(\xi - \xi_0) \end{aligned}\right\} \tag{2b}$$

where p and q are the rates of roll and pitch, respectively, in radians per second, and η_0 and ξ_0 are the distances from the origin of coordinates to the roll axis and the pitch axis, respectively. From equations (1) to (2b) the first, second, and fourth integrals of equation (1) are seen to vanish for the pressure

coefficient due to angle of attack and roll, whereas the second and fourth integrals vanish for the pressure coefficient due to pitch.

It is convenient to convert the required integrals to an oblique coordinate system whose axes are the rearward Mach lines from the origin. The origin of the coordinates is taken at the juncture of the supersonic and subsonic parts of the leading edge. The conversion equations are (fig. 3)

$$u = \frac{M}{2\beta}(\xi - \beta\eta) \qquad v = \frac{M}{2\beta}(\xi + \beta\eta)$$

$$\xi = \frac{\beta}{M}(v + u) \qquad \eta = \frac{1}{M}(v - u)$$

$$u_w = \frac{M}{2\beta}(x - \beta y) \qquad v_w = \frac{M}{2\beta}(x + \beta y)$$

$$x = \frac{\beta}{M}(v_w + u_w) \qquad y = \frac{1}{M}(v_w - u_w) \tag{3}$$

The elementary area in this coordinate system is $\frac{2\beta}{M}\,dudv$. The coordinates (u_w, v_w) or (x,y) are used to represent the point on the wing for which the pressure coefficient is desired, whereas (u,v) or (ξ,η) represent variables of integration. In the oblique coordinate system, the equations for the load distributions due to angle of attack, roll, and pitch become, respectively, (fig. 4)

$$2\frac{\beta}{\alpha}C_p = -\frac{2}{\pi}\frac{\left(1 - \frac{du_3}{dv}\right)}{\sqrt{u_w - u_3}}\int_b^{v_w}\frac{dv}{\sqrt{v_w - v}} - \frac{2}{\pi}\int_a^b \frac{dv - du}{\sqrt{(u_w - u)(v_w - v)}} \tag{4}$$

$$2\frac{U\beta}{p\eta_0}C_p = -\frac{2}{\pi M\eta_0}\frac{\left(1 - \frac{du_3}{dv}\right)}{\sqrt{u_w - u_3}}\int_b^{v_w}\frac{(v - u_3 - M\eta_0)dv}{\sqrt{v_w - v}}$$

$$-\frac{2}{\pi M\eta_0}\int_a^b \frac{(v - u - M\eta_0)(dv - du)}{\sqrt{(u_w - u)(v_w - v)}} \tag{4a}$$

$$2\frac{U\beta}{q\xi_0}C_p = -\frac{2\beta}{\pi M\xi_0}\frac{\left(1-\frac{du_3}{dv}\right)}{\sqrt{u_w-u_3}}\int_b^{v_w}\frac{\left(v+u_3-\frac{M}{\beta}\xi_0\right)dv}{\sqrt{v_w-v}}$$

$$-\frac{2\beta}{\pi M\xi_0}\int_a^b\frac{\left(v+u-\frac{M}{\beta}\xi_0\right)(dv-du)}{\sqrt{(u_w-u)(v_w-v)}}$$

$$-\frac{2\beta}{\pi M\xi_0}\,2\iint_{S_{w,1}}\frac{dudv}{\sqrt{(u_w-u)(v_w-v)}} \qquad (4b)$$

where u_3 and its derivatives are evaluated for $v = v_w$. Equations (4), (4a), and (4b) can be integrated for arbitrary forms of $u_3(v_w)$, if u and v are linearly related along the line $\overline{ab}$. In other words, if the supersonic part of the leading edge is a straight line, explicit expressions for the load distribution are readily obtainable for arbitrary forms of the subsonic leading and trailing edges. If the supersonic leading edge is not a straight line, the load distributions due to angle of attack and roll may still be obtained by means of a simple graphical integration along the required part $\overline{ab}$ of the leading edge. The treatment of such wings to determine the lift distribution is described in detail in reference 5. This method may be readily extended to determine the line integrals along $\overline{ab}$ for load distribution due to roll and pitch. The area integral required for the pitch loading (equation (4b)), although somewhat more difficult to evaluate than the line integrals, is also subject to stripwise, graphical integration methods.

The integrations from b to v_w in equations (4) to (4b) (along the Mach line $u = u_3(v_w)$) are independent of the form of the wing boundary and hence may always be explicitly integrated. If the Kutta-Joukowski condition is imposed at the trailing edge, these integrals need be evaluated only when the right forward Mach line from (u_w,v_w) intersects the plan-form boundary at a subsonic

leading edge $\left(0 < \frac{du_3}{dv} < 1\right)$. If the right forward Mach line intersects the plan-form boundary at a subsonic trailing edge $\left(\frac{du_3}{dv} > 1\right)$, the integrals along $u = u_3(v_w)$ vanish.

The analysis may now be extended to regions of the wing influenced by all its subsonic leading and trailing edges. In general, such regions may be of two types (figs. 5(a) and 5(b)). In both types of region, the left forward Mach line from (u_w,v_w) intersects a subsonic leading or trailing edge at the opposite side of the wing. In figure 5(a), (u_w,v_w) lies in a region of type VI (fig. 1), for which the reflections of the forward Mach lines at the wing boundaries do not intersect on the wing surface. In figure 5(b), (u_w,v_w) lies in a region of type VIII, for which the reflections of the forward Mach lines cross on the wing surface. For both types of region, the methods of reference 1 indicate that an additional line integral along the Mach line $v = v_4(u_w)$ must be added to equation (4). These integrals are the same as those along $u = u_3(v_w)$, except that v replaces u, and v_4 replaces u_3. The sense of the integration is again from the supersonic leading edge v_1 or v_2 to the subsonic edge v_4. The integration along $v = v_4$, like that along $u = u_3$, vanishes (for solutions that satisfy the Kutta-Joukowski condition) if the forward Mach line from (u_w,v_w) intersects a subsonic trailing edge (as it does, for example, in fig. 5(b)).

Along the supersonic leading edge, the sense of the integration is from a to b for both types of region. The values of the line integrals along $\overline{ab}$ are thus of opposite sign for figures 5(a) and 5(b).

The area integrations for the pitch loading (equation (4c)) extend over the shaded areas of figures 5(a) and 5(b). For the type of region shown in figure 5(b), the area integration consists of two parts. The integration over the downstream area is independent of the form of the supersonic leading edge. The integration over the upstream area depends on the contour of the supersonic leading edge. This integration is subtracted from the integration for the lower area, because two area cancelations are involved, one for each of the regions off the two subsonic leading edges (reference 1).

For regions of type VII (fig. 1), both right and left reflected Mach lines intersect the plan-form boundary along the same supersonic leading edge. A point in this region is like a point in region VIII if the Mach lines cross on the surface and is like a point in region VI if the Mach lines do not cross.

For regions of types I and II, both forward Mach lines intersect the plan-form boundary at supersonic leading edges. Hence, all of the line integrals except that along the supersonic leading edge vanish, and the limits for this integral are the points of intersection of the forward Mach lines with the leading edge. The area integration for the pitch loading extends over the region bounded by the forward Mach lines and the leading edge.

APPLICATION TO WINGS WITH STRAIGHT SUPERSONIC LEADING EDGES

When the wing is symmetrical and a section of the leading edge on both sides of the line of symmetry is straight and swept ahead of the Mach lines from the vertex, the equations for the supersonic leading edges are $u_1 = -kv$ and $u_2 = \frac{Mn_0}{k}(1-k) - \frac{v}{k}$. The origin of coordinates is taken at the juncture of the supersonic and subsonic leading edges (fig. 6). The axis of symmetry is identified with the roll axis. For a general region on such a wing, line integrals are required along the Mach lines reflected from the subsonic leading edges and along the two sections of the supersonic leading edge. The limits for these line integrals, as well as those for the area integration required for pitch loading, vary with the type of region considered. The presentation is simplified if the expressions for a general region are first evaluated and the appropriate limits for each region are then indicated.

In the following expressions for the load distributions due to angle of attack, steady roll, and steady pitch, respectively, the first integral is the line integral along $v = v_4(u)$, the second is the integral along $u = u_3(v)$, the third is along $u = u_1(v)$, and the fourth is along $u = u_2(v)$:

$$-\frac{\pi}{2}\left(2\frac{\beta}{\alpha}C_p\right) = \frac{1-\frac{dv_4}{du}}{\sqrt{v_w-v_4}}\int_a^{u_w}\frac{du}{\sqrt{u_w-u}} + \frac{1-\frac{du_3}{dv}}{\sqrt{u_w-u_3}}\int_{c'}^{v_w}\frac{dv}{\sqrt{v_w-v}}$$

$$-\frac{1+k}{k}\int_{b'}^{c}\frac{du}{\sqrt{(u_w-u)\left(v_w+\frac{u}{k}\right)}} - (1+k)\int_{a'}^{b}\frac{du}{\sqrt{(u_w-u)\left[v_w+ku-Mn_0(1-k)\right]}} \qquad (5)$$

$$-\frac{\pi M\eta_0}{2}\left(2\frac{U\beta}{p\eta_0}C_p\right)=\frac{1-\frac{dv_4}{du}}{\sqrt{v_w-v_4}}\int_a^{u_w}\frac{(v_4-u-M\eta_0)du}{\sqrt{u_w-u}}$$

$$+\frac{1-\frac{du_3}{dv}}{\sqrt{u_w-u_3}}\int_{c'}^{v_w}\frac{(v-u_3-M\eta_0)dv}{\sqrt{v_w-v}}+\frac{1+k}{k}\int_{b'}^{c}\frac{\left(\frac{1+k}{k}u+M\eta_0\right)du}{\sqrt{(u_w-u)\left(v_w+\frac{u}{k}\right)}}$$

$$+(1+k)\int_{a'}^{b}\frac{[u(1+k)+kM\eta_0]du}{\sqrt{(u_w-u)[v_w+ku-M\eta_0(1-k)]}} \qquad (5a)$$

$$-\frac{\pi M\xi_0}{2\beta}\left(2\frac{U\beta}{q\xi_0}C_p\right)=\frac{1-\frac{dv_4}{du}}{\sqrt{v_w-v_4}}\int_a^{u_w}\frac{(v_4+u-\frac{M}{\beta}\xi_0)du}{\sqrt{u_w-u}}$$

$$+\frac{1-\frac{du_3}{dv}}{\sqrt{u_w-u_3}}\int_{c'}^{v_w}\frac{(v+u_3-\frac{M}{\beta}\xi_0)dv}{\sqrt{v_w-v}}+\frac{1+k}{k}\int_{b'}^{c}\frac{\left(\frac{1-k}{k}u+\frac{M}{\beta}\xi_0\right)du}{\sqrt{(u_w-u)\left(v_w+\frac{u}{k}\right)}}$$

$$-(1+k)\int_{a'}^{b}\frac{\left[u(1-k)+M\eta_0(1-k)-\frac{M}{\beta}\xi_0\right]du}{\sqrt{(u_w-u)[v_w+ku-M\eta_0(1-k)]}}+2S \qquad (5b)$$

where

$$S = \iint_{S_w} \frac{dudv}{\sqrt{(u_w-u)(v_w-v)}}$$

is the integration over the required areas for each region.

From these integrals, the following explicit expressions are obtained for the load distributions due to angle of attack, steady roll, and steady pitch, respectively:

$$2\frac{\beta}{\alpha}C_p = -\frac{4}{\pi}\left[\left(1-\frac{dv_4}{du}\right)\sqrt{\frac{u_w-a}{v_w-v_4}} + \left(1-\frac{du_3}{dv}\right)\sqrt{\frac{v_w-c'}{u_w-u_3}}\right]$$

$$-\frac{4}{\pi}\frac{1+k}{\sqrt{k}}\left\{\left[\tan^{-1}\sqrt{\frac{u_w-u}{kv_w+u}}\right]_{b'}^{c} + \left[\tan^{-1}\sqrt{\frac{k(u_w-u)}{v_w+ku-M\eta_0(1-k)}}\right]_{a'}^{b}\right\} \quad (6)$$

$$2\frac{U\beta}{p\eta_0}C_p = \frac{4}{\pi M\eta_0}\left[\left(\frac{2}{3}u_w - v_4 + \frac{a}{3} + M\eta_0\right)\left(1 - \frac{dv_4}{du}\right)\sqrt{\frac{u_w-a}{v_w-v_4}}\right.$$

$$\left. - \left(\frac{2}{3}v_w - u_3 + \frac{c'}{3} - M\eta_0\right)\left(1 - \frac{du_3}{dv}\right)\sqrt{\frac{v_w-c'}{u_w-u_3}}\right]$$

$$+ \frac{2}{\pi M\eta_0}\frac{(1+k)^2}{k}\left\{\left[\sqrt{(u_w-u)\left(v_w+\frac{u}{k}\right)}\right]_{b'}^{c} + \left[\sqrt{(u_w-u)\left[v_w+ku-M\eta_0(1-k)\right]}\right]_{a'}^{b}\right\}$$

$$+ \frac{2}{\pi M\eta_0}\frac{1+k}{k^{3/2}}\left[\tan^{-1}\sqrt{\frac{u_w-u}{kv_w+u}}\right]_{b'}^{c}\left[(1+k)(u_w-kv_w) + 2kM\eta_0\right]$$

$$+ \frac{2}{\pi M\eta_0}\frac{1+k}{k^{3/2}}\left[\tan^{-1}\sqrt{\frac{k(u_w-u)}{v_w+ku-M\eta_0(1-k)}}\right]_{a'}^{b}\left[(1+k)(ku_w-v_w) + (1+k^2)M\eta_0\right] \qquad (6a)$$

$$2\frac{U\beta}{q\xi_0}C_p = -\frac{4\beta}{\pi M\xi_0}\left[\left(\frac{2}{3}u_w + v_4 + \frac{a}{3} - \frac{M}{\beta}\xi_0\right)\left(1 - \frac{dv_4}{du}\right)\sqrt{\frac{u_w-a}{v_w-v_4}}\right.$$

$$\left. + \left(\frac{2}{3}v_w + u_3 + \frac{c'}{3} - \frac{M}{\beta}\xi_0\right)\left(1 - \frac{du_3}{dv}\right)\sqrt{\frac{v_w-c'}{u_w-u_3}}\right]$$

$$+ \frac{2\beta}{\pi M\xi_0}\frac{1-k^2}{k}\left\{\left[\sqrt{(u_w-u)\left(v_w+\frac{u}{k}\right)}\right]_{b'}^{c} - \left[\sqrt{(u_w-u)\left[v_w+ku-M\eta_0(1-k)\right]}\right]_{a'}^{b}\right\}$$

$$+ \frac{2\beta}{\pi M\xi_0}\frac{1+k}{k^{3/2}}\left[\tan^{-1}\sqrt{\frac{u_w-u}{kv_w+u}}\right]_{b'}^{c}\left[(1-k)(u_w-kv_w) + 2k\frac{M}{\beta}\xi_0\right]$$

$$- \frac{2\beta}{\pi M\xi_0}\frac{1+k}{k^{3/2}}\left[\tan^{-1}\sqrt{\frac{k(u_w-u)}{v_w+ku-M\eta_0(1-k)}}\right]_{a'}^{b}\left[(1-k)(ku_w-v_w)\right.$$

$$\left. + (1-k^2)M\eta_0 - 2k\frac{M}{\beta}\xi_0\right] - \frac{4\beta}{\pi M\xi_0}S \qquad (6b)$$

The appropriate limits for each of the eight regions shown in figure 6 are given in the following table:

Limit	Wing regions (fig. 6)							
	I	II	III	IV	V	VI	VII	VIII
a	u_w	u_w	u_w	u_w	u_w	$\frac{M\eta_0}{k}(1-k)+$ $-\frac{v_4}{k}$	$\frac{M\eta_0}{k}(1-k)+$ $-\frac{v_4}{k}$	$-kv_4$
a'	u_w	u_w	u_w	u_w	u_w	$\frac{M\eta_0}{k}(1-k)+$ $-\frac{v_4}{k}$	$\frac{M\eta_0}{k}(1-k)+$ $-\frac{v_4}{k}$	u_d
b	u_w	u_d	u_w	u_d	u_3	u_d	u_3	u_3
b'	u_w	u_d	u_w	u_d	u_3	u_d	u_3	$-kv_4$
c	$-kv_w$	$-kv_w$	u_3	u_3	u_3	u_3	u_3	u_d
c'	v_w	v_w	$-u_3/k$	$-u_3/k$	$-ku_3 +$ $M\eta_0(1-k)$	$-u_3/k$	$-ku_3 +$ $M\eta_0(1-k)$	$-ku_3 +$ $M\eta_0(1-k)$

An examination of equations (6) to (6b) shows that the arc-tangent factors are the same for each type of load distribution. The square-root terms are also the same for the roll and pitch loadings. Application of the foregoing table to equations (6) to (6b) shows that many terms vanish for some of the wing regions because the upper and lower limits are identical. The location of these limits for regions of types VI and VIII are shown in figure 5.

The expressions for S in each region are:

Region	Area integration, S
I	$\frac{\pi}{2} A$
II	$\left(\frac{\pi}{2} - C_1\right) A + BC_2$
III	$2C_3 + AC_4$
IV	$2C_3 + A(C_4 - C_1) + BC_2$
V	$2C_5 + BC_6$
VI	$2(C_7 + C_3) + A(C_4 - C_1) + B(C_2 - C_8)$
VII	$2(C_7 + C_5) + B(C_6 - C_8)$
VIII	$2(C_5 + C_{10}) + A(C_1 - C_9) + B(C_6 - C_2)$

where

$$A = \frac{2}{\sqrt{k}} (u_w + kv_w)$$

$$B = \frac{2}{\sqrt{k}} \left[ku_w+v_w-M\eta_0(1-k)\right]$$

$$C_1 = \tan^{-1} \sqrt{\frac{u_w-u_d}{k(v_w-v_d)}}$$

$$C_2 = \tan^{-1} \sqrt{\frac{k(u_w-u_d)}{v_w-v_d}}$$

$$C_3 = \sqrt{(u_w-u_3)(v_w+\frac{u_3}{k})}$$

$$C_4 = \tan^{-1} \sqrt{\frac{u_w-u_3}{kv_w+u_3}}$$

$$C_5 = \sqrt{(u_w-u_3)\left[v_w+ku_3-M\eta_0(1-k)\right]}$$

$$C_6 = \tan^{-1} \sqrt{\frac{k(u_w-u_3)}{v_w+ku_3-M\eta_0(1-k)}}$$

$$C_7 = \sqrt{\left[u_w+\frac{v_4}{k}-\frac{M\eta_0}{k}(1-k)\right](v_w-v_4)}$$

$$C_8 = \tan^{-1} \sqrt{\frac{ku_w+v_4-M\eta_0(1-k)}{v_w-v_4}}$$

$$C_9 = \tan^{-1} \sqrt{\frac{u_w+kv_4}{k(v_w-v_4)}}$$

$$C_{10} = \sqrt{(u_w+kv_4)(v_w-v_4)}$$

Equations (6) to (6b) have been used to calculate the load distributions due to lift, roll, and pitch for the wing shown in figure 7. For computation, use of the coordinates $u_w/M|\eta_0|$ and $v_w/M|\eta_0|$ rather than u_w, v_w was convenient. These coordinates make equations 6 to 6(b) nondimensional.

For the wing shown in figure 7, the ratio $\frac{\beta|\eta_0|}{\xi_0}$ was taken equal to 1.0. The value of k is 1/3. The equations for the subsonic edges were assumed to be

$$\frac{u_3}{M|\eta_0|} = 4\left(\frac{v}{M|\eta_0|}\right)^3$$

$$\frac{v_4}{M|\eta_0|} = 1 + 4\left(\frac{u}{M|\eta_0|} - 1\right)^3 \qquad (7)$$

In order to satisfy the Kutta-Joukowski condition, the integral along $u = u_3$ is zero for $v_w/(M|\eta_0|) > 12^{-1/2}$; and the integral along $v = v_4$ is zero for $u_w/(M|\eta_0|) > 1 + 12^{-1/2}$, because $\frac{du_3}{dv}$ and $\frac{dv_4}{du}$ are then greater than unity.

The contour of the wing is represented in figure 7 for a Mach number of $\sqrt{2}$, although in the (u,v) coordinate system the plot represents a series of wings whose spatial contours vary with Mach number according to equations (7) and the value $k = 1/3$. Hence the load distributions calculated for this wing apply directly to all wings of the series defined by $k = 1/3$ and equations (7). The load distributions for a considerable variety of plan forms, at a given Mach number, can be obtained from the load distributions calculated for the wing of figure 7 by terminating the wing with any form of supersonic trailing edge. The load distributions for the remaining regions of the wing are unaffected by such changes.

The effect of altering the location of the roll or pitch axes can be determined with the aid of the superposition principle. If

the roll and pitch axes are shifted to η_1 and ξ_1, respectively, then equations (2a) and (2b) become, for roll,

$$\sigma_T = -\frac{p}{U}(\eta-\eta_0) - \frac{p}{U}(\eta_0-\eta_1)$$

$$\sigma_B = \frac{p}{U}(\eta-\eta_0) + \frac{p}{U}(\eta_0-\eta_1) \tag{8}$$

and, for pitch,

$$\sigma_T = -\frac{q}{U}(\xi-\xi_0) - \frac{q}{U}(\xi_0-\xi_1)$$

$$\sigma_B = \frac{q}{U}(\xi-\xi_0) + \frac{q}{U}(\xi_0-\xi_1) \tag{8a}$$

Because $\frac{p}{U}(\eta_0-\eta_1)$ and $\frac{q}{U}(\xi_0-\xi_1)$ are constants, the contributions to the load distributions due to these terms are exactly equivalent to the load distributions due to the corresponding angles of attack. Thus, if the load distributions are computed for the axes η_0 and ξ_0 (or for some relation such as $\beta|\eta_0|/\xi_0 = 1$, as assumed for the wing of fig. 7), the load distributions for roll or pitch about any other axes are simply the load distributions for the axes η_0 and ξ_0 plus the lift distributions for the angles of attack:

$$\alpha = \pm\frac{p}{U}(\eta_0-\eta_1)$$

and

$$\alpha = \pm\frac{q}{U}(\xi_0-\xi_1)$$

For a family of wings whose contour is represented by the value $k = 1/3$, and equation (7), the load distributions due to angle of attack, steady roll, and steady pitch are shown in figures 8, 9, and 10, respectively. The dashed lines in these figures are Mach lines that separate the various regions indicated in figure 7. The additional Mach lines at $u_w/(M|\eta_0|) = 1.29$ and at $v_w/(M|\eta_0|) = 0.29$ separate the regions influenced by the subsonic

trailing edges from those influenced only by leading edges. The pressure coefficient is zero along the subsonic trailing edge for each type of loading, because the Kutta-Joukowski condition was imposed in each case. Along each subsonic leading edge the pressure coefficient is infinite.

The lift distribution shows that positive lift exists on all parts of the wing surface except the extreme rearward tip (region VIII and part of region VII). This negative region is a result of the upwash over the subsonic edges. The lift decreases rapidly toward the subsonic edges. The region of the wing having the highest lift is that bounded by the leading edges and by the Mach lines from the beginning of the trailing edges.

For steady roll (fig. 9), the loading is negative in the outboard part of region IV and in nearly all of regions V, VI, and VII. In region VIII, the loading again becomes positive. The large negative region results because the greatest contribution to the loading proceeds from the leading edge on the opposite side of the wing, where the vertical component of the perturbation velocity is of opposite sign.

The load gradient for steady pitch (fig. 10) is primarily in the chordwise direction, except in the regions influenced largely by subsonic trailing edges. High positive loading occurs toward the front of the wing and high negative loading toward the rear. The loading becomes negative ahead of the pitch axis because the contribution due to the area integration and the contribution due to the line integrals are of opposite sign ahead of the pitch axis ($\xi_0 > \xi$). The loading therefore changes sign when the contribution of the integrals over the area included in the forward Mach cone is sufficiently large to overbalance the contribution due to the line integrals.

SUMMARY OF THEORY AND RESULTS

A method has been presented for determining the load distribution due to steady roll and steady pitch on thin wings whose plan form is arbitrary except that a part of the leading edge must be supersonic. When the supersonic part of the leading edge is a straight line, these load distributions can be explicitly evaluated for all regions of the wing except those influenced by interacting flow fields off the plan form.

For a particular family of wings having a plan form that includes most types of flow field commonly encountered, the load distributions due to angle of attack, steady roll, and steady pitch

were computed. The lift distribution for this family of wings showed that negative lift may exist toward the rear of pointed wings if the aspect ratio is small. The highest lift occurred in regions affected only by leading edges. In steady roll, negative loading occurred in regions influenced by the edge of the plan form at the opposite side of the roll axis. At the extreme rear of a low-aspect-ratio wing, the loading again became positive. With the pitch axis located near the semichord position, the load gradient for steady pitch was primarily in the chordwise direction except in regions influenced by subsonic trailing edges. High positive loading occurred toward the front of the wing and high negative loading toward the rear.

Flight Propulsion Research Laboratory,
National Advisory Committee for Aeronautics,
Cleveland, Ohio, May 15, 1948.

REFERENCES

1. Evvard, John C.: The Theoretical Distribution of Lift on Thin Wings at Supersonic Speeds (An Extension). NACA TN No. 1585, 1948.

2. Evvard, John C., and Turner, L. Richard: Theoretical Lift Distribution and Upwash Velocities for Thin Wings at Supersonic Speeds. NACA TN No. 1484, 1947.

3. Brown, Clinton E., and Adams, Mac C.: Damping in Pitch and Roll of Triangular Wings at Supersonic Speeds. NACA TN No. 1566, 1948.

4. Jones, Arthur L., and Alksne, Alberta: The Damping Due to Roll of Triangular, Trapezoidal, and Related Plan Forms in Supersonic Flow. NACA TN No. 1548, 1948.

5. Cohen, Clarence B., and Evvard, John C.: A Graphical Method of Obtaining the Theoretical Lift Distribution on Thin Wings Moving at Supersonic Speeds. NACA TN No. 1676, 1948.

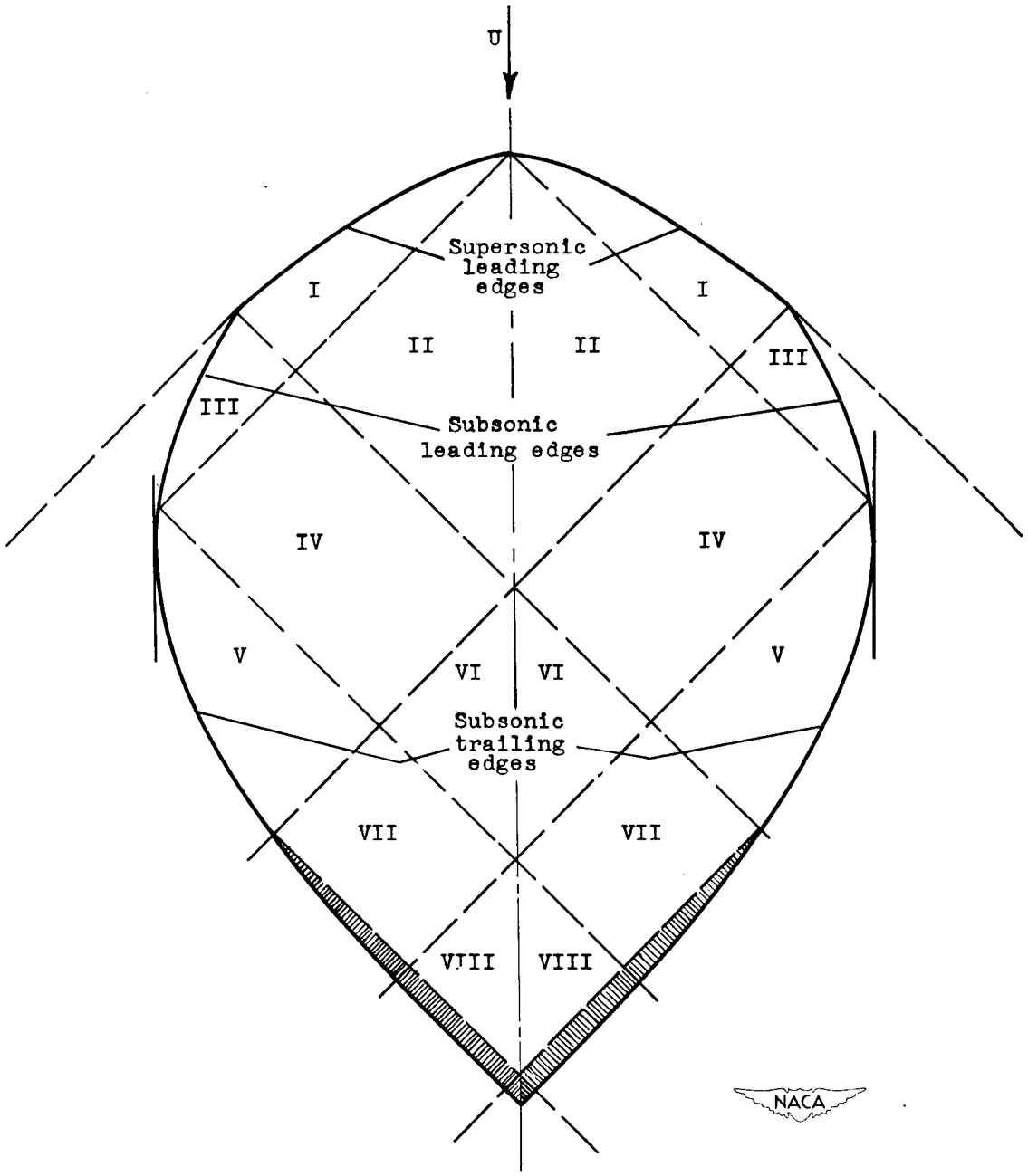

Figure 1. - Types of wing region commonly encountered at supersonic speeds.

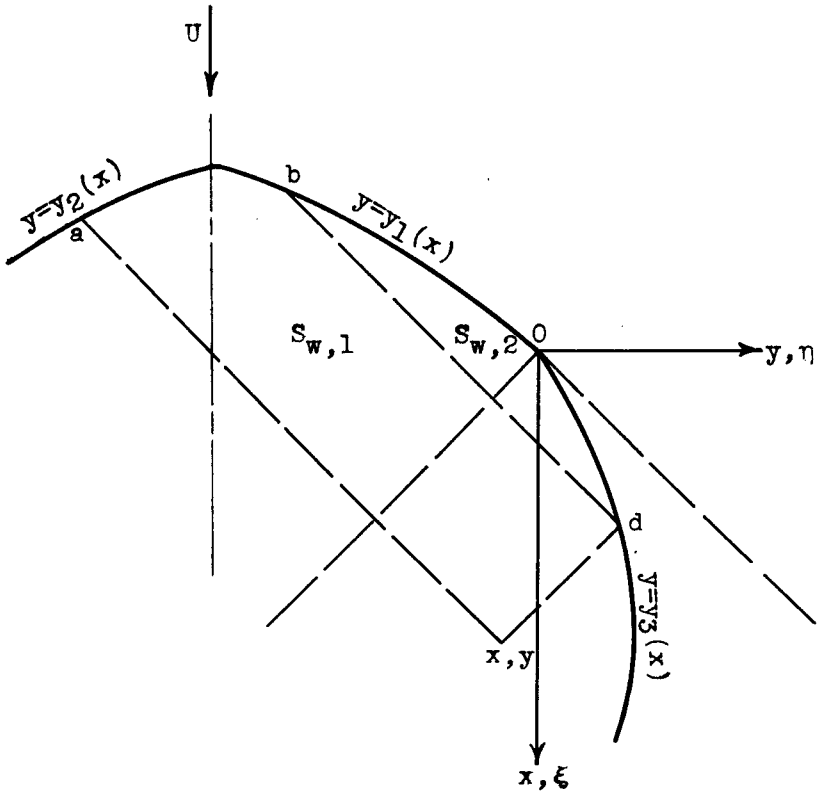

Figure 2. - Illustration of geometric significance of equation (1).

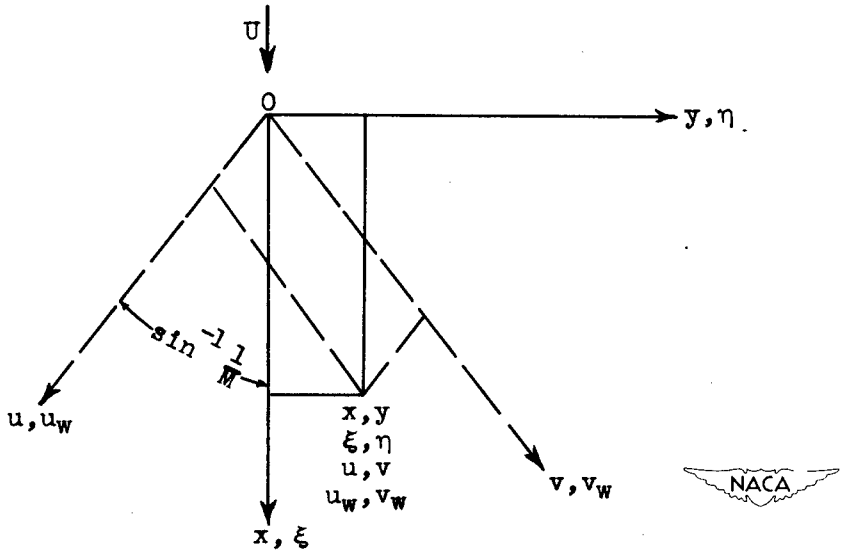

Figure 3. - Relation between Cartesian and oblique coordinate systems.

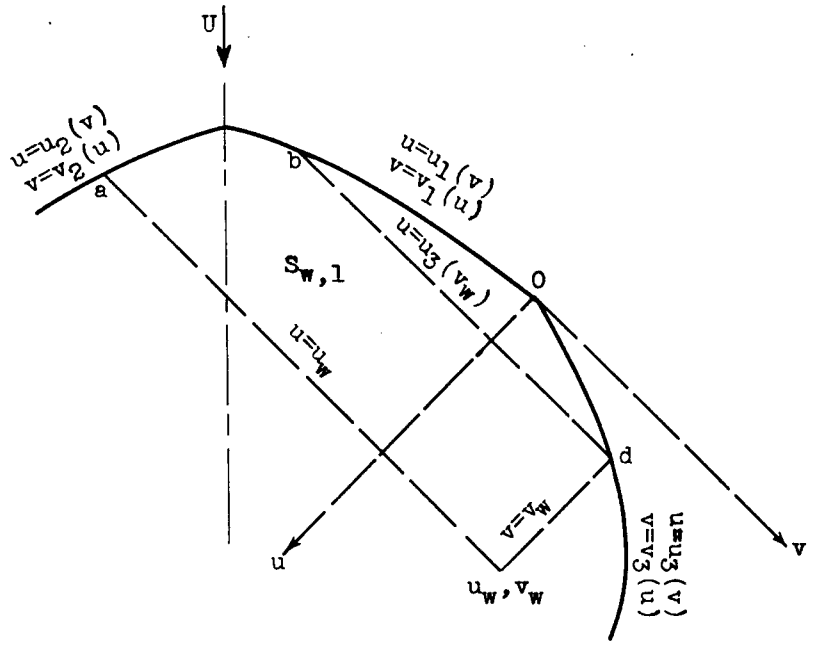

Figure 4. - Illustration of geometric significance of equations (4).

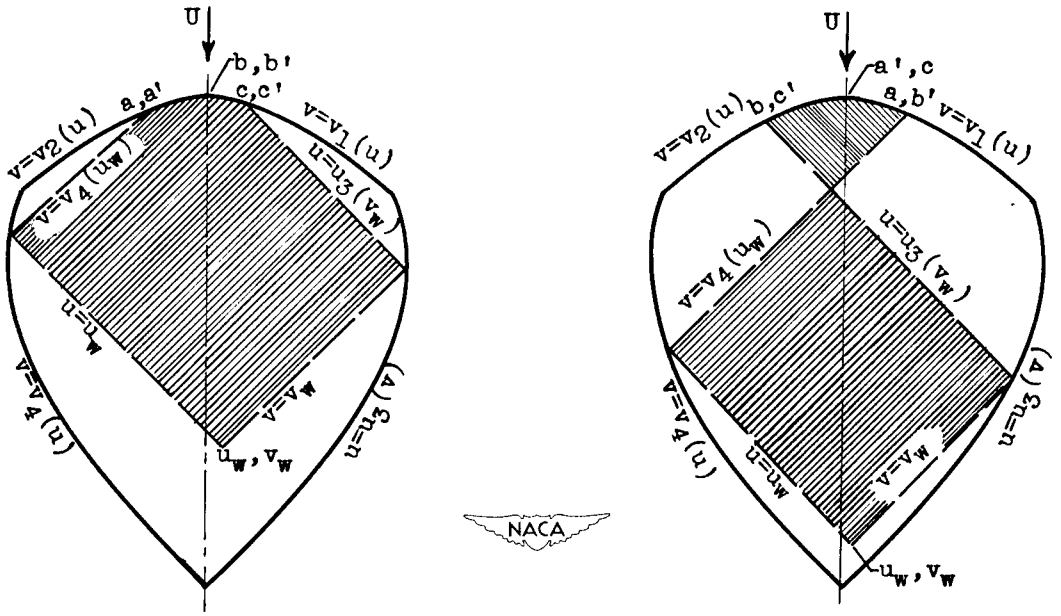

(a) Reflected forward Mach lines do not intersect on surface.

(b) Reflected forward Mach lines intersect on surface.

Figure 5. - Two types of wing region influenced by two subsonic edges.

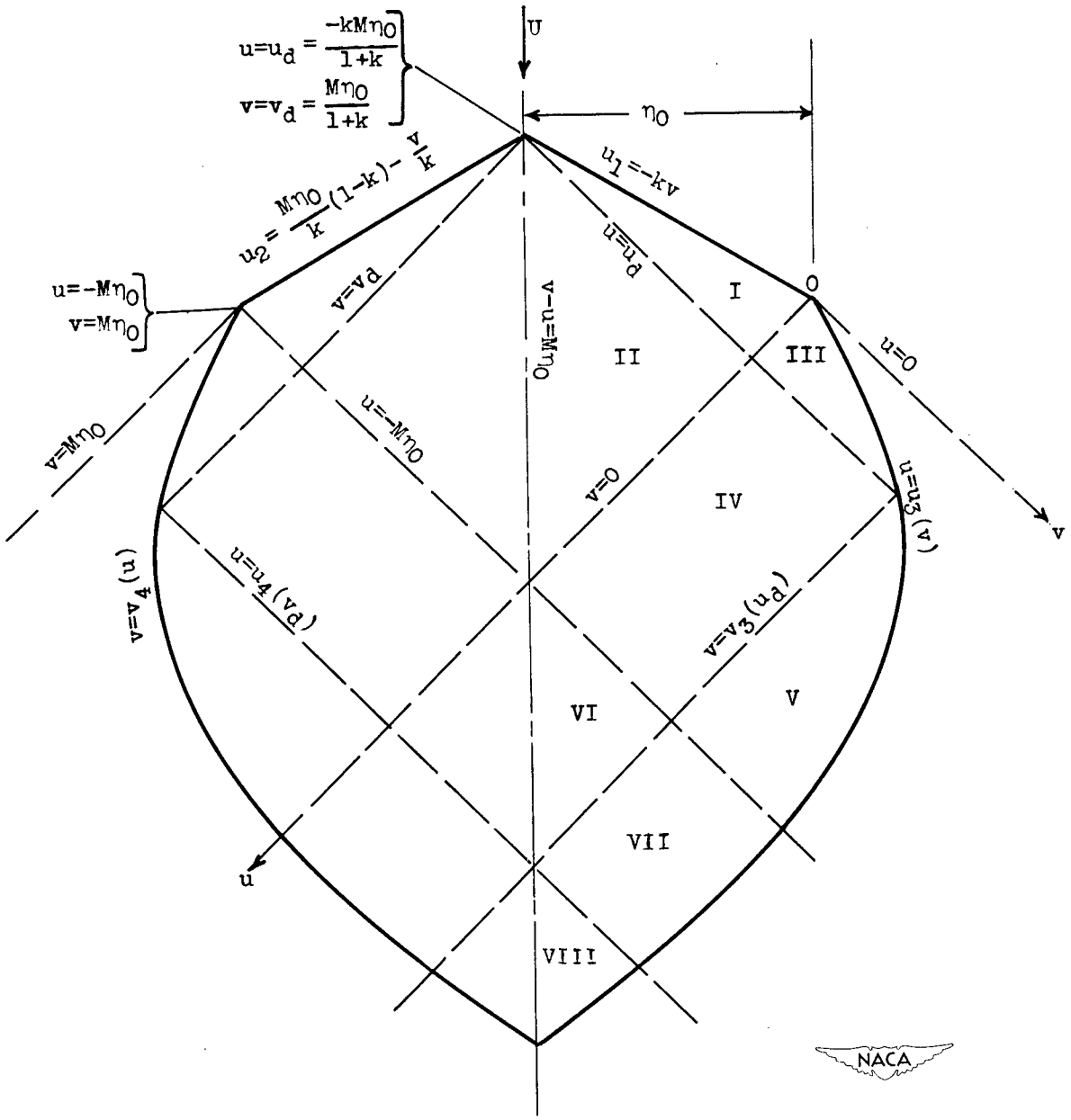

Figure 6. - Geometric parameters for symmetrical wing with straight supersonic leading edges and arbitrary subsonic leading and trailing edges.

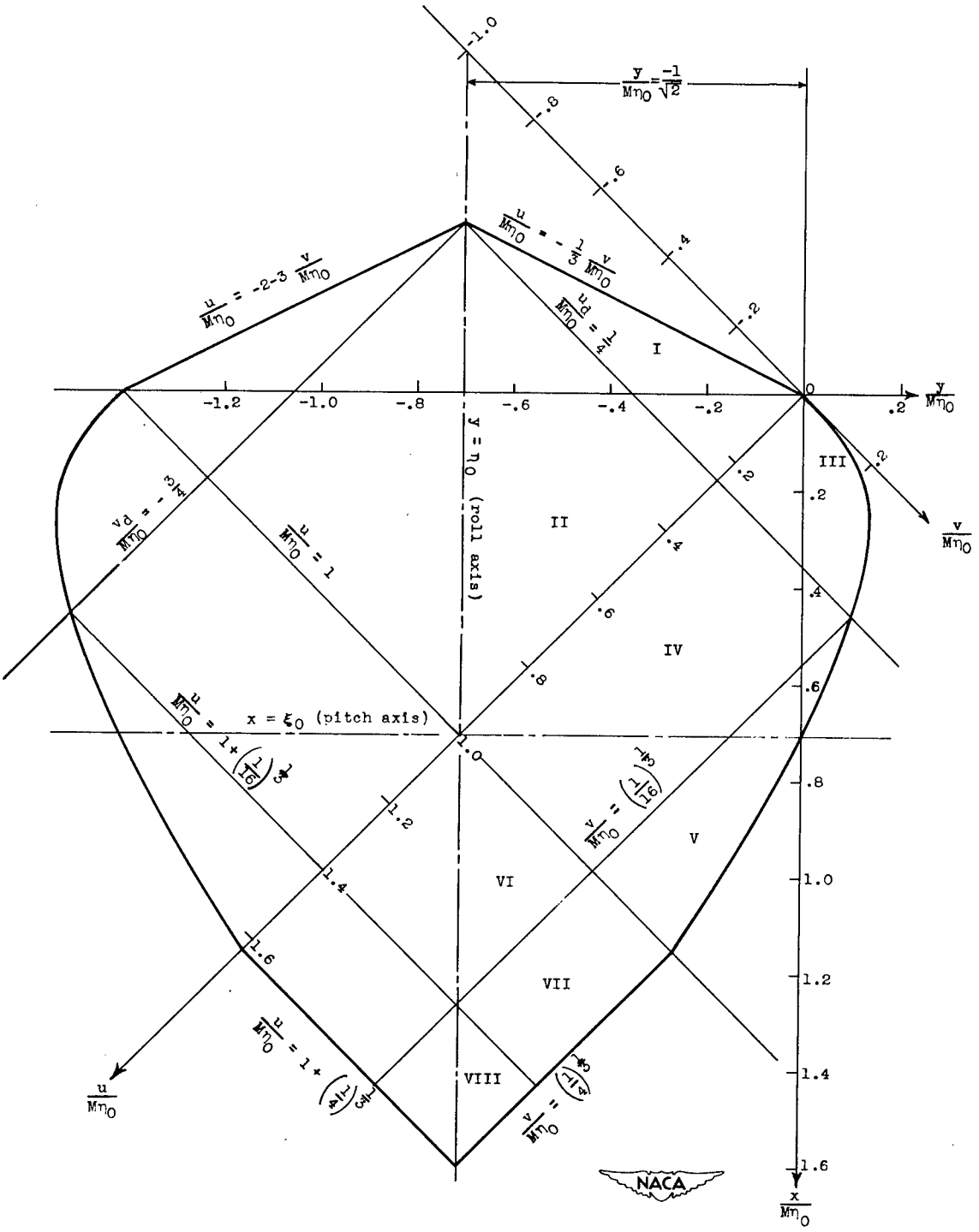

Figure 7. - Form of wing analyzed. $M = \sqrt{2}$.

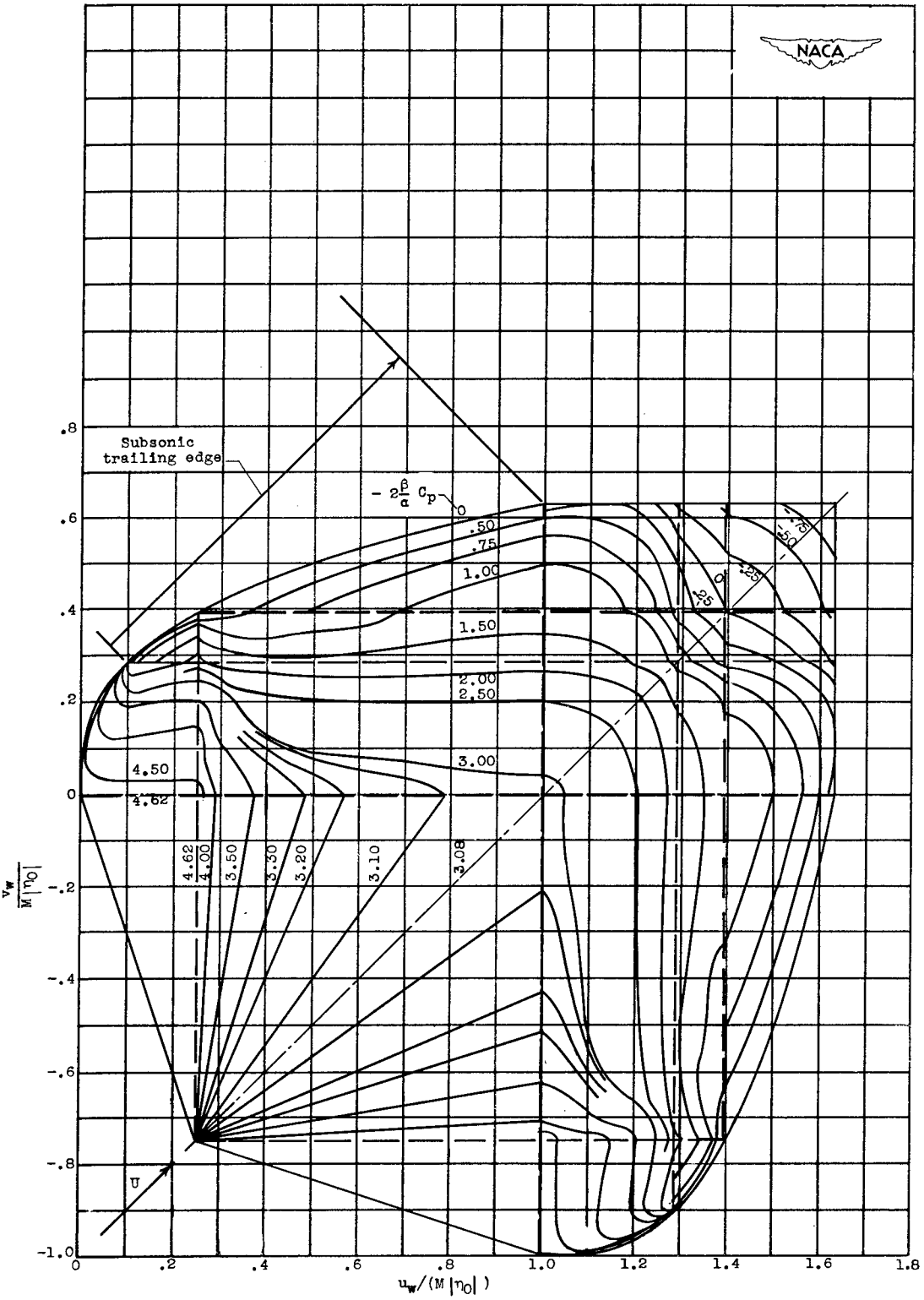

Figure 8. - Lift distribution for series of wings defined by $k = 1/3$ and equations (7).

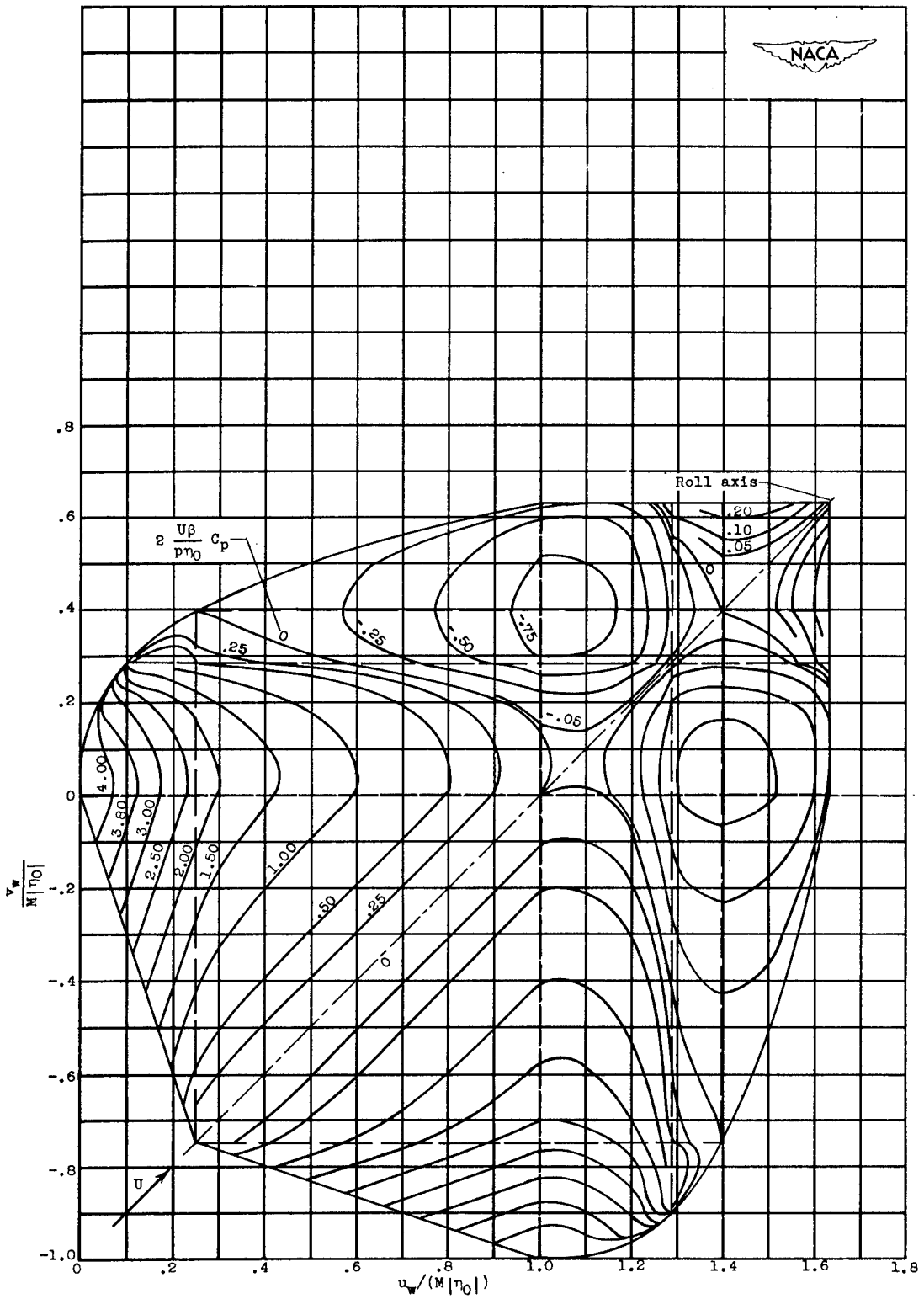

Figure 9. - Load distribution in steady roll for wing defined by $k = 1/3$ and equations (7).

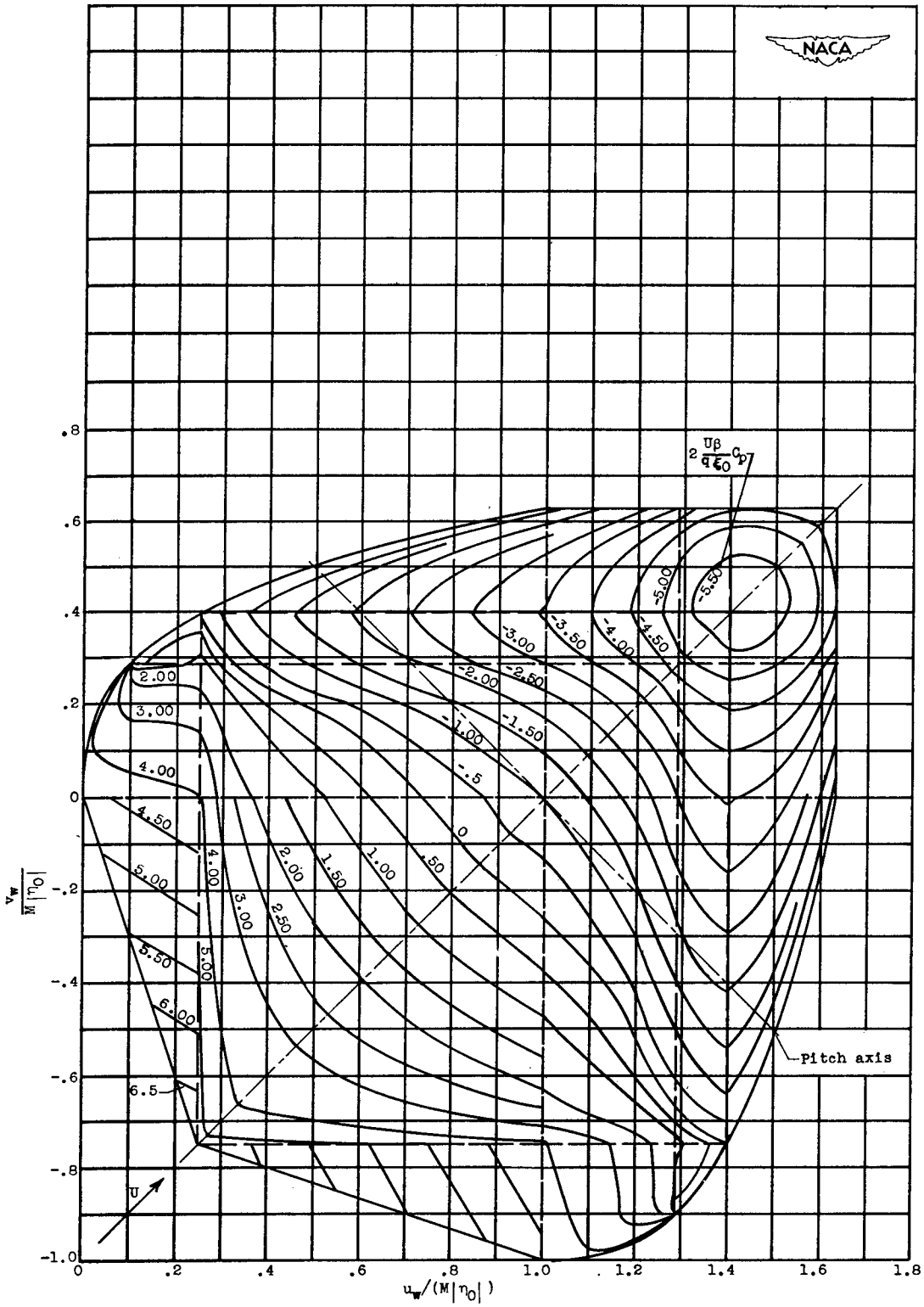

Figure 10. - Load distribution in steady pitch for wing defined by k = 1/3 and equations (7).